中國機械工程學刊第四十一卷第二期第 159~168 頁(民國一百零九年)
Journal of the Chinese Society of Mechanical Engineers, Vol.41, No.2, pp 159~168 (2020)

Stiffness Model of Bolted Joint of Machine Tool Based on Multi-scale Theory

Cheng Yang*, Yong-Sheng Zhao**, Zhi-Feng Liu** and Li-Gang Cai**

Keywords：dynamic performance, bolted joint, multi-scale theory, frequency level, CNC machine tool.

ABSTRACT

Computer numerical controlled (CNC) machine tools are comprised of numerous parts mainly connected by bolts. Accurate modeling of the contact stiffness of bolted joints is therefore a crucial element in predicting the dynamic performance of CNC machine tools. This paper presents a contact stiffness model of a bolted joint based on multi-scale theory. The model uses a series of stacked three-dimensional sine waves to describe the multi-scale roughness of the contact surface, and each frequency level is considered to be a single layer of asperities, which are stacked on top of each other. A relationship between the contact area ratio and frequency level can be deduced. Moreover, the contact stiffness at each frequency level can be represented within the model as a spring in series, therefore, the total stiffness is obtained by summing the contact stiffness at each frequency level. An experimental setup consisting of a box-shaped specimen was used to validate the numerical model of the bolted joint for the case of equal bolt pre-tightening forces and relative errors between the multi-scale natural frequencies and experimental frequencies were found to be less than 5.91%. This suggests the multi-scale model can be used to effectively predict the dynamic characteristics of CNC machine tools.

INTRODUCTION

The dynamic behavior of bolted joints has an important influence on the precision of computer numerical controlled (CNC) machine tools. Many factors affect the dynamic behavior including the surface roughness, pre-tightening forces on each bolt, and material properties (Mao et al., 2010). Since the surfaces of most engineering materials are characteristically rough, they can be considered multi-scale surfaces presenting multiple non-uniform asperities. Hence, an appropriate contact model is necessary to accurately predict the dynamic behavior of the joint surface.

Over the past few years, a number of contact models have been presented to describe bolted joints. One of the earliest proposed models is that of Greenwood and Williamson (GW) (Greenwood et al., 1966). Some assumptions are necessary in the GW model, for instance, all asperities with the same curvature and Gaussian or exponential distributions are assumed to be evenly spaced, as well as any point of contact between neighboring asperities. The relationship between the total real contact area and nominal contact pressure can then be deduced using appropriate statistical methods. Shi et al. (2012) introduced a contact stiffness model based on a specific formula for determining the number of asperities, and obtained parameters describing the contact surface based on GW contact theory. Other extensions of the GW model consider the effects of both plastic and adhesion deformation (Kogut et al., 2002; Zhao et al., 2000; Jackson et al., 2005). However, the statistical roughness parameters used in the GW model and related models depend on the length scale, therefore most models are limited by the instruments available to obtain these measurements. Furthermore, applying the GW model to realistic surfaces is often difficult due to the random topographies of various surfaces.

Fractal theory has been widely adopted to study engineering surfaces and offers features such as independent measurements and self-affinity. Majumdar et al. (1990) presented the famous M-B fractal contact model and identified the relationship between the total real contact area and normal load using the W-M function and Hertz theory. A normal contact stiffness model based on fractal theory and Hertz contact theory, independent of scale, was

Paper Received February, 2018. Revised July, 2018. Accepted October, 2018. Author for Correspondence: Yong-Sheng Zhao.

* *Gradnate Student, Beijing Key Laboratory of advanced manufacturing technology, Beijing University of Technology, Beijing 100124, China.*

** *Professor, Beijing Key Laboratory of advanced manufacturing technology, Beijing University of Technology, Beijing 100124, China.*

previously established by Zhang et al. (2000) for joint surfaces, modeled as a sphere and rigid plane. Jiang et al. (2010) determined the contact stiffness of bolted joints under different contact loads using three different machining methods. Moreover, Komvopoulos et al. (2002) performed a comprehensive finite element method (FEM) analysis of elastic-plastic contact to model real surfaces exhibiting fractal behavior. Furthermore, Zhao et al. (2016) established a contact stiffness and damping model based on the nonlinear virtual material method and uneven surface contact pressure distribution method. A number of additional studies have investigated fractal-based contact models (Borri-Brunetto et al., 2001; Komvopoulos et al., 2001; Willner et al., 2006; Wang, 2011). However, the fractal contact model is only effective when contact surfaces are under light load conditions.

Recently, multi-scale theory has been used to study the contact mechanism of bolted joints in order to address the multi-scale characteristics of rough machined surfaces. The so-called “protuberance upon protuberance” multi-layer rough surface model was presented by Archard (1957) and simulates multi-scale surface roughness as numerous small-scale spherical asperities superimposed on large-scale spherical asperities. Wilson et al. (2010) proposed a multi-scale model based on superimposing the sine function. Compared to the existing statistics-based contact models, the multi-scale model was shown to be closer to the actual situation and unaffected by the resolution of measurement systems. Furthermore, Ciavarella et al. (2000) applied Archaed's protuberance upon protuberance multi-layer rough surface model to solve contact problems between a two-dimensional fractal surface and rigid rough surface based on the W-M function and obtained a formula for contact resistance.

The Fourier series was used by Jackson and Streator (2006) to represent different scales of rough surface asperities and a multi-scale normal contact model, also non-statistical, was proposed. Based on the model, it was concluded that real contact areas vary linearly with load regardless of whether the contact is elastic or elasto-plastic. The sinusoidal contact model was further studied by Krithivasan and Jackson (2007), who investigated the effects of plasticity on individual asperities. Instead of using previous asymptotic methods, Johnson, Greenwood, and Higginson (JGH) (1985) used exact solutions based on Hertz contact theory to propose a more realistic rough surface contact model. Fewer stiffness models of the contact surface based on multi-scale theory have been presented. Therefore, the main objective of this paper is to describe the contact stiffness of a bolted joint based on a multi-scale model and to deduce the relationship between the contact area ratio and frequency level.

The MATRIX27 element was introduced into the finite element model of the bolted assembly in order to define the normal and tangential contact stiffness of the joint surface. In addition, two box-shaped specimens connected by bolts were set up to validate the model. Numerical and experimental mode shapes and natural frequency values were compared, and relative errors between the multi-scale natural frequencies and experimental frequencies were found to be less than 5.91%. This suggests the proposed multi-scale model could be used to accurately predict the dynamic characteristics of bolted assemblies in CNC machine tools.

MULTI-SCALE MODEL OF JOINT SURFACE

The contact stiffness of bolted joints can have a significant influence on the dynamic performance of CNC precision machining, therefore an accurate model of contact stiffness is required to successfully predict the dynamic performance of CNC machine tools. The proposed multi-scale model uses a series of stacked three-dimensional (3D) sine waves to describe the multi-scale roughness of the contact surface, as shown in Figure 1. The multi-scale parameters of the contact surface topography can be obtained by applying the fast Fourier transform (FFT) to the rough surface profile, however, a few simplifying assumptions are necessary (Jackson et al., 2006; Goedecke et al., 2013), as follows:

(1) Asperities of different frequency levels are assumed to be stacked on top of each other.

(2) Each frequency level supports the same total load, moreover, all asperities share the load equally since they are assumed to have the same height at a given frequency level.

(3) At a given frequency level, Hertz contact theory or an appropriate elastic-plastic contact model is applied to determine the deformation of each asperity, while all other asperities are assumed to have negligible influence.

(4) The real contact area at a given frequency level cannot be larger than the contact area of the frequency level below it.

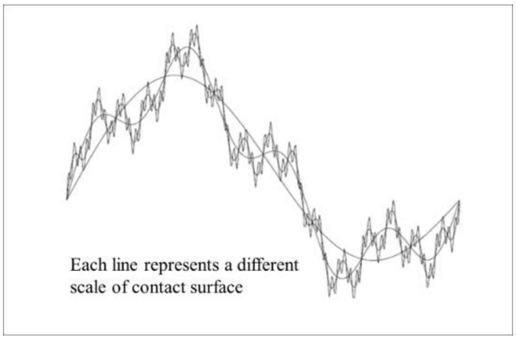

Fig. 1. Representative multi-scale model of a rough surface.

This paper adopts the multi-scale model proposed by Jackson and Streator (2006). The contact surface is considered to be the summation of a series of sine waves. The real contact area is denoted by A_r and the nominal contact area is A_n, therefore, the equations of the multi-scale contact model can be expressed as

$$A_r = (\prod_{i=1}^{i_{max}} \bar{A}_i \eta_i) A_n \tag{1}$$

$$F = \bar{F}_i \eta_i A_{i-1} \tag{2}$$

where F is the total contact force and $\bar{A}_i$ denotes the contact area, $\bar{F}_i$ denotes the contact force, and η_i is the areal asperity density at a given frequency level i, and $i_{\max}$ is the maximum frequency level. The areal asperity density and asperity radius of curvature can be calculated by applying FFT to the rough surface profile at each frequency level, expressed as

$$\eta_i = 2 f_i^2 \tag{3}$$

$$R_i = \frac{1}{4\pi^2 \beta_i f_i^2} \tag{4}$$

where β_i and f_i are the amplitude and frequency, respectively, at frequency level i and A_n is the nominal contact area when i is zero.

STIFFNESS MODEL OF BOLTED JOINT BASED ON MULTI-SCALE THEORY

Normal stiffness model of bolted joint

The multi-scale geometry model is one of the best-known models for describing mechanical surfaces. The multi-scale model uses a series of stacked sine waves to describe the multi-scale roughness of the joint surface. When two rough surfaces are held in contact by high strength bolts under different pre-tightening forces, elastic-plastic deformation of the asperities occurs. Based on the definition of contact stiffness, elastic-plastic deformation can be related to simple elastic deformation. When asperities only undergo plastic deformation, the contact stiffness is zero. Hertz contact theory can be applied to a perfectly elastic contact between two rough surfaces. According to the JGH model, at a given frequency level i and for a small load, $\bar{F}_i << F_i^*$, the contact area of a single asperity can be given by

$$(\bar{A}_i)_1 = \frac{\pi}{2 f_i^2} \left\{ \frac{3}{8\pi} \frac{\bar{F}_i}{F_i^*} \right\}^{\frac{2}{3}} \tag{5}$$

where F_i^* is the average pressure required at frequency level i for complete contact between the surfaces. However, as the load is increased, complete contact is almost realized as $\bar{F}_i$ approaches F_i^*, such that the contact area of a single asperity can be given by

$$(\bar{A}_i)_2 = \frac{1}{f_i^2} \left(1 - \frac{3}{2\pi} \left[1 - \frac{\bar{F}_i}{F_i^*} \right] \right) \tag{6}$$

where F_i^* is defined as

$$F_i^* = \sqrt{2}\pi E' \beta_i f_i \tag{7}$$

Jackson and Streator (2006) defined a linking equation for determining the asymptote solutions of Eqs. (5) and (6) based on the experimental and numerical data of the JGH model, which can be expressed as follows:

For $\bar{F} / F_i^* < 0.8$,

$$\bar{A}_i = (\bar{A}_i)_1 \left(1 - \left(\frac{\bar{F}_i}{F_i^*} \right)^{1.51} \right) + (\bar{A}_i)_2 \left(\frac{\bar{F}_i}{F_i^*} \right)^{1.04} \tag{8}$$

And for $\bar{F} / F_i^* \geq 0.8$,

$$\bar{A}_i = (\bar{A}_i)_2 \tag{9}$$

The pressure acting on the individual asperities increases as the total load increases, eventually causing the asperity material to yield at the bolted joint. Then, many asperities at different frequency levels undergo plastic deformation. Therefore, an elasto-plastic sinusoidal contact model that considers this effect, such as the one presented in this paper, is required. At a given frequency level, the critical interference $(\omega_c)_i$ at the initial point of yielding can be derived based on the von Mises yield criterion, as demonstrated by Jackson and Green, is expressed as

$$(\omega_c)_i = \left(\frac{\pi C S_y}{2E'} \right)^2 R_i \tag{10}$$

where S_y is the yield strength of the material, C is the critical yield stress coefficient, and E' is the equivalent elastic modulus, which are given by

$$C = 1.295 \exp(0.736\nu) \tag{11}$$

$$\frac{1}{E'} = \frac{1-\nu_1^2}{E_1} + \frac{1-\nu_2^2}{E_2} \tag{12}$$

where ν refers to the Poisson's ratio of the material that yields first, ν_1 and ν_2 are the Poisson's ratios of the two surfaces, and E_1 and E_2 are the corresponding elastic moduli.

The critical force $(\bar{F}_c)_i$ at a given frequency level calculated at the critical interference can be written as

$$(\bar{F}_c)_i = \frac{4}{3} \left(\frac{R_i}{E'} \right)^2 \left(\frac{C\pi S_y}{2} \right)^3 \tag{13}$$

Similarly, the critical contact area $(\bar{A}_c)_i$ at frequency level i can be expressed as

$$(\bar{A}_c)_i = \pi^3 \left(\frac{C S_y R_i}{2E'} \right)^2 \tag{14}$$

As previously stated, when $\bar{F}_i \ll F_i^*$ at a given frequency level *i*, asperities in contact exhibit perfect elastic behavior. However, as the load increases to a critical value, plastic deformation will occur. To evaluate the plastic deformation of an asperity at a given frequency level *i*, Eq. (5) can be replaced by another equation (Wilson et al., 2000) to obtain

$$(\bar{A}_i)_p = 2\left((\bar{A}_c)_i\right)^{\frac{1}{1+q}}\left(\frac{3\bar{F}_i}{4CS_y f_i^2}\right)^{\frac{q}{1+q}} \tag{15}$$

$$q = 3.8\left(\frac{E'}{S_y}\beta_i f_i\right)^{0.11} \tag{16}$$

Then, the contact area at frequency level *i* becomes

$$\bar{A}_i = (\bar{A}_i)_p\left(1-\left[\frac{\bar{F}_i}{F_{iP}^*}\right]^{1.51}\right) + (\bar{A}_i)_2\left(\frac{\bar{F}_i}{F_{iP}^*}\right)^{1.04} \tag{17}$$

Furthermore, the pressure required to achieve complete contact during elastic-plastic deformation can be written as

$$\frac{F_{iP}^*}{F_i^*} = \left(\frac{11}{4\beta_i/\Delta\beta + 7}\right)^{\frac{3}{5}} \tag{18}$$

$$\Delta\beta = \frac{\sqrt{2}S_y \exp(\frac{2\nu}{3})}{3\pi E' f_i} \tag{19}$$

where $\Delta\beta$ is the critical amplitude at a given frequency level *i*, below which the sine wave will always undergo elastic deformation and adding more pressure will cause plastic deformation. The critical amplitude can be determined when the maximum von Mises stress is equal to the yield strength.

For the case of elastic deformation of an asperity, contact force $\bar{F}_i$ and contact area a_i of a single asperity at a given frequency level *i* can be determined using Hertz contact theory, and are expressed as

$$\bar{F}_i = \frac{4}{3}E' R_i^{\frac{1}{2}}\omega_i^{\frac{3}{2}} \tag{20}$$

$$a_i = \pi r_i^2 = \pi R_i \omega_i \tag{21}$$

where ω_i is the interference between the surfaces and r_i is the contact radius of a single asperity.

According to Eqs. (20) and (21), r_i can be expressed as

$$r_i = \left(\frac{3\bar{F}_i R_i}{4E'}\right)^{\frac{1}{3}} \tag{22}$$

By definition, the normal contact stiffness $(k_n)_i$ of each elastic asperity at a given frequency level *i* can be expressed as

$$(k_n)_i = \frac{d\bar{F}_i}{d\omega_i} = 2E' R_i^{\frac{1}{2}}\omega_i^{\frac{1}{2}} = 2E' r_i \tag{23}$$

According to Eqs. (23), (4), and (22), the contact stiffness $(k_n)_i$ of a single asperity at a given frequency level can be written as

$$(k_n)_i = 2E'\left(\frac{3\bar{F}_i}{8\pi^2 E'\beta_i\eta_i}\right)^{\frac{1}{3}} \tag{24}$$

The number of asperities can be defined as N_i at a given frequency level *i*. Then, according to the definition we obtain $\bar{F}_i = F/N_i$ and $\bar{A}_i = A_i/N_i$. Thus, the total stiffness $(K_n)_i$ at frequency level *i* can be written as

$$(K_n)_i = N_i (k_n)_i = \eta_i A_{i-1}(k_n)_i \tag{25}$$

Substituting Eq. (24) into Eq. (25), the solution becomes

$$(K_n)_i = 2\eta_i A_{i-1} E'\left(\frac{3\bar{F}_i}{8\pi^2 E'\beta_i\eta_i}\right)^{\frac{1}{3}} = 2E'^{\frac{2}{3}}\left(\frac{3FA_{i-1}^2 f_i^2}{4\pi^2\beta_i}\right)^{\frac{1}{3}} \tag{26}$$

Elastic deformation occurs when $\bar{A}_i < (\bar{A}_c)_i$ at a given frequency level *i*. The contact area and critical frequency level i_c for elastic deformation to occur can be calculated at frequency level *i*. At frequency level $i+1$, plastic deformation will occur. Then, i_c can be defined as the critical frequency level and the critical contact area $(\bar{A}_c)_i$ can be expressed as

$$(\bar{A}_c)_i = \pi^3\left(\frac{CS_y R_i}{2E'}\right)^2 = \frac{1}{\pi}\left(\frac{CS_y}{8E'\beta_i f_i^2}\right)^2 \tag{27}$$

Jackson and Streator (2006) represented an iterative relationship for determining the real contact area between a given frequency level and the frequency level just below, as follows:

$$\frac{A_i}{A_n} = \frac{1}{4}\left(\frac{9}{2\pi}\right)^{\frac{1}{3}}\left(\frac{F}{E'A_n}\right)^{\frac{2}{3}}\left(\frac{1}{f_i\beta_i}\right)^{\frac{2}{3}}\left(\frac{A_{i-1}}{A_n}\right)^{\frac{1}{3}} \tag{28}$$

The multi-scale parameters f and β at different frequency levels can be computed using the following equation:

$$\beta_i = \alpha\left(\frac{1}{f_i}\right)^{\gamma} \tag{29}$$

where both α and γ are constants derived from the Fourier series of the surface data.

According to Eqs. (26), (28), and (29), the contact stiffness at a given frequency level *i* can be obtained when the frequency level is less than the critical frequency level i_c, and the model can be regarded as a model consisting of springs in series. Therefore, total stiffness K_n can be expressed as

$$\frac{1}{K_n} = \sum_{i=1}^{i_c}\frac{1}{(K_n)_i} \tag{30}$$

Tangential stiffness model of bolted joint

Asperities will deform in the shear direction when a tangential force acts on the contact surface under a normal load. According to reference (Kogut et al., 2002), the tangential deformation of a single asperity at a given frequency level can be written as

$$t_i = \frac{3}{16\bar{G}r_i} e\bar{F}_i \left\{ 1 - \left[1 - \frac{\bar{Q}_i}{e\bar{F}_i} \right]^{\frac{2}{3}} \right\} \tag{31}$$

where e refers to the static friction coefficient, G and E are the shear modulus and elastic modulus of the material, respectively, $\bar{G}$ denotes the equivalent shear modulus of the two contact surface, G_1 and G_2 are the shear modulus of the two respective contact surfaces, $\bar{Q}_i$ is the tangential load acting on a single asperity at given frequency level. The static friction coefficient can be defined as

$$e = \left(\frac{G}{E} \right)^{\frac{1}{2}} \tag{32}$$

Moreover, the shear modulus can be expressed as

$$\bar{G} = \left(\frac{2-\nu_1}{G_1} + \frac{2-\nu_2}{G_2} \right)^{-1} \tag{33}$$

By definition, the tangential contact stiffness $(k_t)_i$ for each asperity at a given frequency level i can be expressed as

$$(k_t)_i = \frac{d\bar{Q}_i(t_i)}{dt_i} = 8\bar{G}r_i \left(1 - \frac{16\bar{G}r_i}{3e\bar{F}_i} t_i \right)^{\frac{1}{2}} \tag{34}$$

Substituting Eq. (31) into Eq. (34), we obtain

$$(k_t)_i = 8\bar{G}r_i \left(1 - \frac{\bar{Q}_i}{e\bar{F}_i} \right)^{\frac{1}{3}} \tag{35}$$

For a single asperity, the relationship between the shear force and normal force can be expressed as

$$\frac{\bar{Q}_i}{\bar{F}_i} = \frac{Q}{F} \tag{36}$$

where Q refers to the tangential force of the contact surface, defined as $Q = \tau A_r$, and τ refers to the shear strength of the softer of the two materials in contact. Then, the tangential contact stiffness of a single asperity corresponding to a given frequency level can be expressed as

$$(k_t)_i = 8\bar{G}r_i \left(1 - \frac{Q}{eF} \right)^{\frac{1}{3}} \tag{37}$$

The total stiffness $(K_t)_i$ at a given frequency level i can be written as

$$(K_t)_i = (k_t)_i N_i = 8\bar{G} \left(1 - \frac{Q}{eF} \right)^{\frac{1}{3}} \left(\frac{3FA_{i-1}^2 f_i^2}{4\pi^2 E' \beta_i} \right)^{\frac{1}{3}} \tag{38}$$

Similar to the normal stiffness model, the total tangential stiffness K_t is given by

$$\frac{1}{K_t} = \sum_{i=1}^{i_{max}} \frac{1}{(K_t)_i} \tag{39}$$

EXPERIMENTAL VALIDATION OF MULTI-SCALE MODEL

A box-shaped specimen was used to experimentally validate the accuracy of the proposed multi-scale model. The in-plane dimensions of the specimen are shown in Figure 2. The material is nodular cast iron (QT600-3, China) and its properties are presented in Table 1. Specimens were machined by grinding to a roughness of Ra = 1.6 μm. A flowchart of the model validation process is illustrated in Figure 3.

Table 1. Material properties of bolted joint

Material parameter	Parameter value
Elastic modulus, E	1.5×10^{11} Pa
Density, ρ	7800 Kg/m^3
Poisson's ratio	0.28

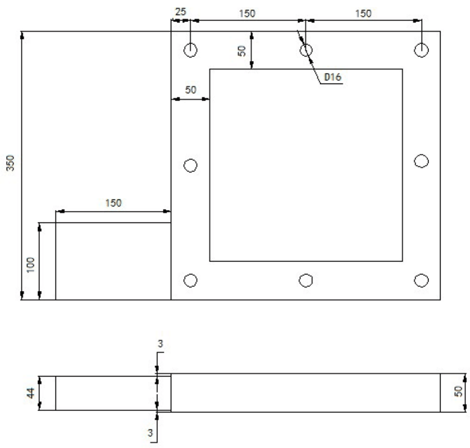

Fig. 2. Plane dimensions of box-shaped specimen

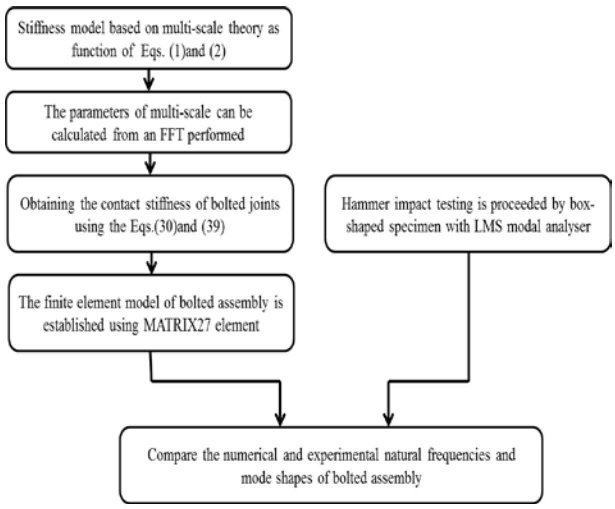

Fig.3. Flowchart of model validation process

Two identical specimens were used in contact tests of the bolted joint connected using eight M16 bolts, as depicted in Figure 4. The assembly was suspended by a rope to simulate the free degree of freedom (DOF) state to eliminate the effects of external forces. Two groups of piezoelectric acceleration sensors (330B30, PCB Piezotronics) were placed on the specimens with a total of nine sensors on each surface of the assembly. An impact hammer was used to provide the excitation signal at the end of one of the specimens. To reduce random error, eliminate the influence of noise, and improve the signal-to-noise ratio, average values were calculated based on three separate experiments. The excitation and sensor signals were collected by LMS modal analyzers and further analyzed on a desktop computer. The LMS modal analyzers can be adopted to offer a complete, integrated solution for test-based engineering that combines high speed 32-channel data acquisition with a full suite of integrated testing, analysis, and reporting tools.

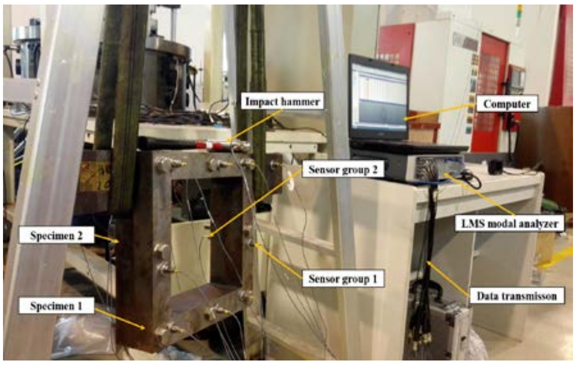

Fig. 4. Contact model tests of bolted joint

Modal analysis of the assembly was performed in ANSYS and a finite element model was established to verify the effectiveness of the multi-scale model of the bolted joint, as illustrated in Figure 5(a). The numbers 1 to 8 represent different positions of the bolts and each bolt was loaded with the same pre-tightening force. A grid model with 1019 nodes was used as the contact interface, and two surfaces have identical meshes so that the nodes are in one-to-one correspondence on two surfaces, which makes it possible to add the self-defined element between two nodes, as shown in Figure 5(b). The surface-to-surface contact element "CONTAC174" is used to define the contact surfaces of bolted joint. The pre-tightening force of each bolt is implemented in the finite element model. All nodes of the contact interface were selected, and the corresponding contact pressure of each node was determined by performing a static analysis. Finally, the contact stiffness of each node was calculated in MATLAB based on the corresponding contact pressure. Here, the MATRIX27 element was adopted to establish the node-node stiffness matrix of the joint surface. One node pair of the MATRIX27 stiffness element is given by

$$\begin{bmatrix} K_x & 0 & 0 & 0 & 0 & 0 & -K_x & 0 & 0 & 0 & 0 & 0 \\ 0 & K_y & 0 & 0 & 0 & 0 & 0 & -K_y & 0 & 0 & 0 & 0 \\ 0 & 0 & K_z & 0 & 0 & 0 & 0 & 0 & -K_z & 0 & 0 & 0 \\ 0 & 0 & 0 & 0 & 0 & 0 & 0 & 0 & 0 & 0 & 0 & 0 \\ 0 & 0 & 0 & 0 & 0 & 0 & 0 & 0 & 0 & 0 & 0 & 0 \\ 0 & 0 & 0 & 0 & 0 & 0 & 0 & 0 & 0 & 0 & 0 & 0 \\ -K_x & 0 & 0 & 0 & 0 & 0 & K_x & 0 & 0 & 0 & 0 & 0 \\ 0 & -K_y & 0 & 0 & 0 & 0 & 0 & K_y & 0 & 0 & 0 & 0 \\ 0 & 0 & -K_z & 0 & 0 & 0 & 0 & 0 & K_z & 0 & 0 & 0 \\ 0 & 0 & 0 & 0 & 0 & 0 & 0 & 0 & 0 & 0 & 0 & 0 \\ 0 & 0 & 0 & 0 & 0 & 0 & 0 & 0 & 0 & 0 & 0 & 0 \\ 0 & 0 & 0 & 0 & 0 & 0 & 0 & 0 & 0 & 0 & 0 & 0 \end{bmatrix}$$

where K_x and K_y refer to tangential stiffness of the X and Y axes, respectively, and K_z denotes the normal stiffness of the joint surface.

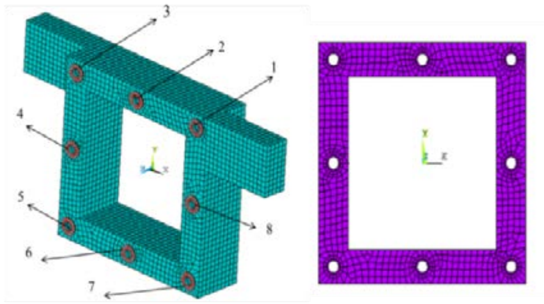

(a) Grid model of bolted joint (b) Grid model of interface

Fig. 5. Grid models of the bolted joint and interface

A stylus profilometer was used to measure the surface profile, which was then used to obtain the parameters used in the multi-scale model, as shown in Figure 6(a). The surface profile consisted of 19 600 data points. The power spectral density of the surface profile generated by FFT is shown in Figure 6(b). The computed power spectral density is sufficiently small, suggesting the physical meaning is lost at higher frequencies.

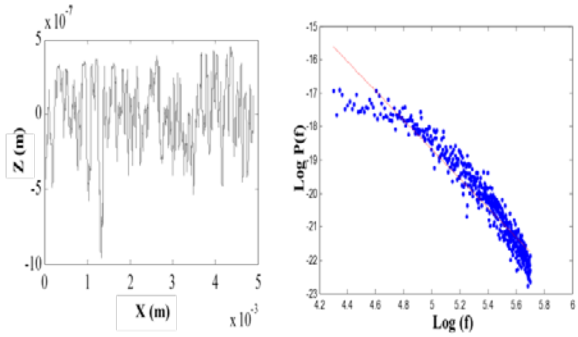

Fig. 6. (a) Surface profile for Ra=1.6 μm (b) Power spectral density of the surface

The power spectrum density method, based on Eq. (29), was used to obtain the constants α=0.026 and γ=1.42 . For F = 18 kN, the relationship between the contact area ratio and frequency level is shown in Figure 7. It can clearly be seen that a few of the lower frequency values play a significant role in changing the contact area ratio, whereas the higher frequency values seem to have little influence. As the frequency level increases, the real contact area decreases, and at frequency levels greater than 50, changes in the contact area ratio are so small that the influence of frequency is negligible. The results agree with the previous predictions of Ciavarella et al. (2000) and suggest that as the frequency level increases, the real contact area tends toward zero.

Table 2. Comparison of the simulated and experimental mode shapes

Simulated	**Experimental**	**Simulated**	**Experimental**
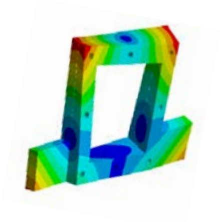	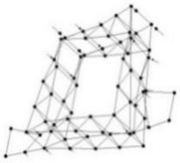	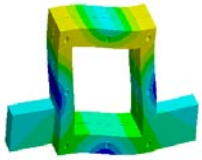	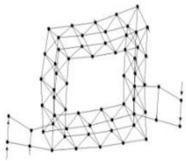
1st order		**2nd order**	
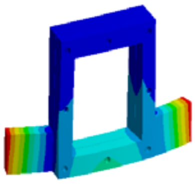	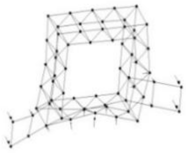	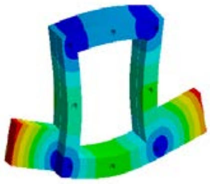	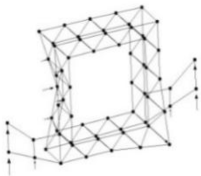
3rd order		**4th order**	
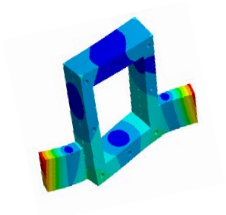	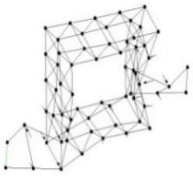	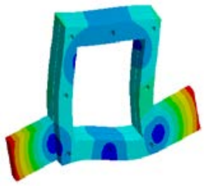	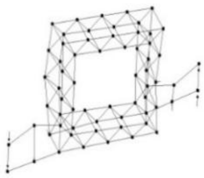
5th order		**6th order**	

Table 3. Natural frequencies of the bolted joint obtained using the multi-scale model (Hz)

		1	**2**	**3**	**4**	**5**	**6**
9 kN	Experiment	533.56	666.09	864.07	869.58	1334.41	1421.03
	Simulation (proposed model)	536.54	627.30	841.73	885.95	1290.70	1383.10
	Error (%)	**0.56**	**-5.82**	**-2.59**	**1.89**	**-3.28**	**-2.67**
	Simulation (ignoring the influence of bolted joints)	556.74	612.60	825.13	830.55	1260.90	1473.10
	Error (%)	**4.34**	**-8.03**	**-4.51**	**-4.49**	**-5.51**	**3.66**
12 kN	Experiment	548.50	665.10	875.30	899.30	1384.00	1416.00
	Simulation (proposed model)	544.56	625.80	861.60	893.10	1317.20	1410.00
	Error (%)	**-0.72**	**-5.91**	**-1.57**	**-0.69**	**-4.83**	**-0.42**
	Simulation (ignoring the influence of bolted joints)	561.06	615.80	821.60	863.10	1282.20	1449.00
	Error (%)	**2.29**	**-7.41**	**-6.14**	**-4.03**	**-7.36**	**2.33**
15 kN	Experiment	552.84	668.28	883.37	900.25	1387.80	1438.90
	Simulation (proposed model)	556.45	635.92	871.88	894.73	1353.30	1434.50
	Error (%)	**0.65**	**-4.84**	**-1.30**	**-0.61**	**-2.49**	**-0.31**
	Simulation (ignoring the influence of bolted joints)	565.26	620.92	821.88	854.73	1283.30	1474.50
	Error (%)	**2.25**	**-7.09**	**-6.97**	**-5.06**	**-7.53**	**2.47**
18 kN	Experiment	562.84	668.57	884.17	900.81	1390.95	1451.00
	Simulation (proposed model)	559.23	686.02	898.12	915.95	1359.90	1456.70
	Error (%)	**-0.64**	**2.61**	**1.58**	**1.68**	**-2.23**	**0.39**
	Simulation (ignoring the influence of bolted joints)	551.96	646.02	822.12	855.95	1302.71	1477.90
	Error (%)	**-1.93**	**-3.37**	**-7.02**	**-4.98**	**-6.34**	**1.85**

The first to 6th order mode shapes of the assembly, measured by hammer impact testing, were compared with the corresponding numerical modal shapes, presented in Table 2. Each bolt was subjected to the same pre-tightening force during the experiments. The finite difference method (Wang et al., 2013) was used to verify the results of the simulation, and mode shapes predicted using the multi-scale method are shown to be similar to the experimental mode shapes (Table 2).

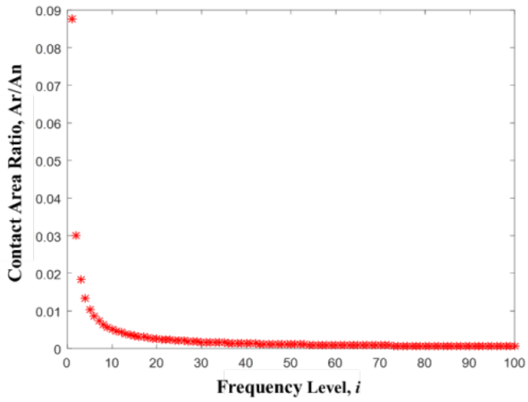

Fig.7. Contact area ratio versus frequency level

The first to 6th order natural frequencies of the assembly obtained using the multi-scale model under different pre-tightening loads are presented in Table 3. To ensure the error of the pre-tightening force of each bolt was than 0.1 kN, experiments were performed three times. For the multi-scale model, relative errors between the natural frequencies obtained using the multi-scale model and experimental frequencies were less than 5.91%. The maximum error was 5.91% for the 2nd order natural frequency with a pre-tightening force of 12 kN. The minimum error was 0.31% for the 6th order natural frequency with a 15 kN pre-tightening force on each bolt. These results were also compared with the model that does not consider the influence of joint surfaces, and the error of the proposed model was found to be smaller. Therefore, the multi-scale theoretical model can effectively predict the dynamic behavior of bolted joints.

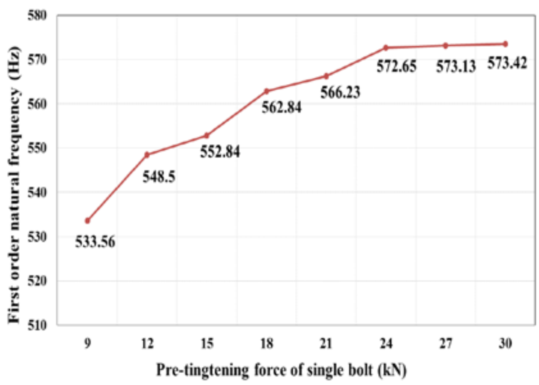

Fig. 8. First order natural frequency versus pre-tightening force

The relationship between the first order natural frequency and pre-tightening force is shown in Figure 8. As the pre-tightening force increases, the first order natural frequency also increases, however, once the pre-tightening force exceeds 24 kN, very little change in the natural frequency is observed. The fundamental reason is that incremental changes in the contact pressure of the bolted assembly occur close to the bolts, whereas further away from the bolts, the contact pressure remains relatively constant. The results suggest the multi-scale method may be useful in optimizing the number of bolts in bolted assemblies and for determining appropriate pre-tightening forces.

CONCLUSIONS

In this paper, a multi-scale model was presented for determining the normal and tangential stiffness of the contact surface of a bolted joint. The iterative multi-scale framework was used to model the contact between two rough surfaces. The results clearly show that a few of the lower frequency values have an important influence on the contact area ratio, however, higher frequencies seem to have little influence on contact area. At frequency levels greater than 50, changes in the contact area ratio are so small that the influence of frequency can be neglected.

Using the proposed multi-scale model, relationships between the stiffness of the bolted joint, multi-scale parameters, and contact area were deduced. Relative errors between the numerical natural frequencies and experimental values were less than 5.91%, thus demonstrating that the multi-scale model can accurately predict the dynamic behavior of bolted joints in CNC machine tools. These results provide a theoretical basis for the optimized design and manufacture of heavy machine tools systems that are affected by the coupling effects of bolted joints.

ACKNOWLEDGMENT

This research was financially supported by National Natural Science Foundation of China (No. 51375025), National Science and Technology Major Project of China (No. 2015ZX04014-021).

REFERENCES

Mao, K., Li B., Wu, J., "Stiffness Influential Factors-based Dynamic Modeling and Its Parameter Identification Method of Fixed Joints in Machine Tools," *International Journal of Machine Tools & Manufacture*, Vol. 50, pp. 156-164 (2010).

Greenwood, J.A., and Williamson, J.B.P., "Contact of Nominally Flat Surfaces," *Proceedings of the Royal Society A Mathematical Physical &*

Engineering Sciences, Vol. 295, pp. 300-319 (1966).
Shi, J.P., Ma, K., and Liu,Z.Q., "Normal Contact Stiffness on Unit Area of A Mechanical Joint Surface Considering Perfectly Elastic Elliptical Asperities," *Journal of Tribology*, Vol. 134, pp. 1-6 (2012).
Kogut, L., and Etsion, I., "Elastic-plastic Contact Analysis of A Sphere and A Rigid Flat," *Journal of Applied Mechanics*, Vol. 69, pp. 657-662 (2002).
Zhao, Y., Maietta, D.M., and Chang L., "An Asperity Microcontact Model Incorporating the Transition from Elastic Deformation to Fully Plastic Flow," *Journal of Tribology*, Vol. 122, pp. 86-93 (2000).
Jackson, R.L., and Green I., "A Finite Element Study of Elastic-plastic Hemi-spherical Contact," *Journal of Tribology*, Vol. 127, pp. 343-354 (2005).
Majumdar, A., and Bhushan, B., "Role of Fractal Geometry in Roughness Characterization and Contact Mechanics of Surfaces," *Journal of Tribology*, Vol. 112, pp. 205-216 (1990).
Zhang, X.L., Huang, Y.M., and Han, Y., "Fractal Model of the Normal Contact Stiffness of Machine Joint Surfaces Based on the Fractal Contact Theory," *China Mechanical Engineering*, Vol. 11, pp. 727-729 (2000).
Jiang, S., Zheng, Y., and Zhu, H., "A Contact Stiffness Model of Machined Plane Joint Based on Fractal Theory," *Journal of Tribology*, Vol. 132, (2010).
Komvopoulos, K., and Ye, N., "Elastic–plastic Finite Element Analysis for the Head-disk Interface with Fractal Topography Description," *Journal of Tribology*, Vol. 124, pp. 775–784 (2002).
Zhao, Y., Yang, C., and Cai, L.G., "Surface Contact Stress-based Nonlinear Virtual Material Method for Dynamic Analysis of Bolted Joint of Machine Tool," *Precision Engineering*, Vol. 43, pp. 230-240 (2016).
Borri-Brunetto, M., Chiaia, B., and Ciavarella M., "Incipient Sliding of Rough Surfaces in Contact: A Multiscale Numerical Analysis," *Computer Methods in Applied Mechanics & Engineering*, Vol. 190, pp. 6053-6073 (2001).
Komvopoulos, K., and Ye N., "Three-dimensional Contact Analysis of Elastic-plastic Layered Media with Fractal Surface Topographies," *Journal of Tribology*, Vol. 123, pp. 632-640 (2001).
Willner, K., "Elasto-plastic Contact of Fractal Surfaces Using Half-space Theory," *Journal of Tribology*, Vol. 27, pp. 305-312 (2006).
Wang, S., "Interfacial Stiffness Characteristic Modeling of Mechanical Fixed Joints," *Journal of Huazhong University of Science & Technology*, Vol. 39, pp. 1-5 (2011).
Archard, J.F., "Elastic Deformation and the Laws of Friction," *Proceedings of the Royal Society A Mathematical Physical & Engineering Sciences*, Vol. 243, pp. 190-205 (1957).
Wilson, W.E., Angadi, S.V., and Jackson, R.L., "Surface Separation and Contact Resistance Considering Sinusoidal Elastic–plastic Multi-scale Rough Surface Contact," *Wear*, Vol.268, No.1, pp.190-201 (2010).
Ciavarella, M., "Linear Elastic Contact of the Weierstrass Profile," *Proceedings of the Royal Society A*, Vol. 456, pp.387-405 (2000).
Jackson, R.L., and Streator J L. "A Multi-scale Model for Contact Between Rough Surfaces," *Wear*, Vol. 261, pp. 1337-1347 (2006).
Krithivasan V., and Jackson, R.L., "An Analysis of Three-dimensional Elasto-plastic Sinusoidal Contact," *Tribology Letters*, Vol. 27, pp. 31-43 (2007).
Johnson, K.L., Greenwood, J.A., and Higginson, J.G., "The Contact of Elastic Regular Wavy Surfaces," *International Journal of Mechanical Sciences*, Vol. 27, pp. 383-396 (1985).
Goedecke, A., Jackson, R.L., and Mock, R., "A Fractal Expansion of A Three Dimensional Elastic–plastic Multi-scale Rough Surface Contact Model," *Tribology International*, Vol. 59, pp. 230-239 (2013).
Wilson, W.E., Angadi, S.V., and Jackson R L., "Surface Separation and Contact Resistance Considering Sinusoidal Elastic–plastic Multi-scale Rough Surface Contact," *Wear*, Vol. 268, pp. 190-201 (2007).
Wang, C.C., and Yau, H.T., "Bifurcation Analysis of Bearing Number in Ultra Short Gas Bearing System," *Smart Science*, pp.18-24 (2013).

NOMENCLATURE

A_r the real contact area

A_n the nominal contact area

$\bar{A}_i$ the contact area at a given frequency level

$\bar{F}_i$ the contact force at a given frequency level

η_i the areal asperity density

i, i_c frequency level and critical frequency level

$i_{\max}$ highest frequency level

F the total contact force

f_i β_i the frequency and amplitude at a given frequency level i

F_i^* the average pressure for complete contact

ω_i, the interference

$(\omega_c)_i$ the critical interference

S_y the yield strength of the material

C the critical yield stress coefficient

E' the equivalent elastic modulus

ν Poisson's ratio of the first material to yield

ν_1, ν_2 Poisson's ratios of the surfaces

E_1, E_2 the elastic moduli of the surfaces

$(\bar{F}_c)_i$ the critical force at a given frequency level

$(\bar{A}_i)_p$ the contact area during plastic deformation

$\Delta\beta$ the critical amplitude at a given frequency level i

a_i the contact area of a single asperity

r_i the contact radius of a single asperity

$(k_n)_i$, $(k_t)_i$ the normal contact stiffness and tangential contact stiffness for each asperity

N_i number of asperities at a given frequency level i

$(K_n)_i$, $(K_t)_i$ the total normal stiffness and total stiffness at a given frequency level i

α, γ the constants derived from the Fourier series

K_n, K_t the total normal and tangential stiffness

t_i the tangential deformation of a single asperity

e the static friction coefficient

G, E the shear modulus and elastic modulus of the material

$\bar{G}$ the equivalent shear modulus of two surfaces

G_1, G_2 the shear modulus of the two contact surfaces

$\bar{Q}_i$ the tangential load acting on a single asperity

Q the Tangential force of the contact surface

τ the shear strength of the softer material

$(\bar{A}_c)_i$ the critical contact area

基于多尺度理論數控機床栓接結合部建模研究

楊成 趙永勝 劉志峰 蔡力鋼
北京工業大學先進制造與智能制造技術研究所

摘 要

數控機床有不同部件通過栓接的形式組合而成，精確的栓接結合部剛度模型對數控機床的動態特性有重要影響。本文提出了一種基于多尺度理論的栓接結合部剛度模型，此模型使用一系列疊加的三維正弦波來表征粗糙接觸表面多尺度特性，每個正弦波被認爲是一層頻率級，推導出了接觸面積比與頻率級的函數關系，則整體剛度可以看作不同頻率級串聯的彈簧模型，接觸總剛度爲各頻率級剛度之和。最後，設計框型試驗件驗證模型的准確性，結果表明多尺度理論模型與試驗結果之間的最大誤差 5.91%，證明多尺度剛度模型能夠有效地預測數控機床的動態特性。